

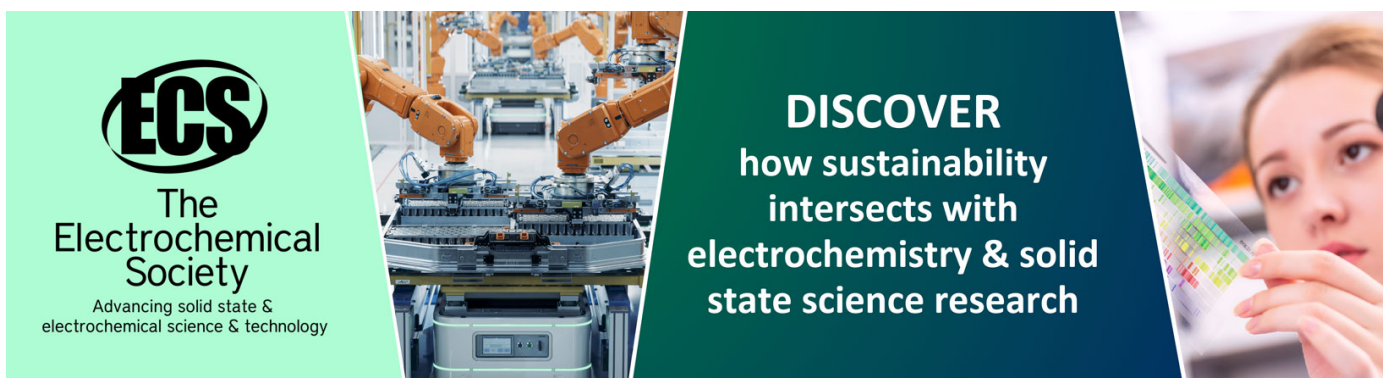
## A single-sided micromachined piezoresistive SiO<sub>2</sub> cantilever sensor for ultra-sensitive detection of gaseous chemicals

To cite this article: Peng Li and Xinxin Li 2006 *J. Micromech. Microeng.* **16** 2539

View the [article online](#) for updates and enhancements.

### You may also like

- [Precisely controlled batch-fabrication of highly sensitive co-resonant cantilever sensors from silicon-nitride](#)  
Ioannis Lampouras, Mathias Holz, Steffen Strehle et al.
- [Review of scaling effects on physical properties and practicalities of cantilever sensors](#)  
C-K Yang, E W J M van der Drift and P J French
- [Integrated microcantilevers for high-resolution sensing and probing](#)  
Xinxin Li and Dong-Weon Lee



**ECS**  
The  
Electrochemical  
Society  
Advancing solid state &  
electrochemical science & technology

**DISCOVER**  
how sustainability  
intersects with  
electrochemistry & solid  
state science research

# A single-sided micromachined piezoresistive SiO<sub>2</sub> cantilever sensor for ultra-sensitive detection of gaseous chemicals

Peng Li<sup>1</sup> and Xinxin Li<sup>1,2,3</sup>

<sup>1</sup> Research Institute of Micro/Nano Science and Technology, Shanghai Jiao Tong University, Shanghai 200030, People's Republic of China

<sup>2</sup> State Key Laboratory of Transducer Technology, Shanghai Institute of Microsystem and Information Technology, Chinese Academy of Sciences, Shanghai 200050, People's Republic of China

E-mail: [xxli@mail.sim.ac.cn](mailto:xxli@mail.sim.ac.cn)

Received 17 August 2006

Published 18 October 2006

Online at [stacks.iop.org/JMM/16/2539](http://stacks.iop.org/JMM/16/2539)

## Abstract

This paper presents a novel SiO<sub>2</sub> microcantilever sensor for high-sensitive gaseous chemical detection. A thin single-crystalline silicon piezoresistor is integrated in the SiO<sub>2</sub> cantilever for low-noise and high-resoluble signal readout. The paper relates the MEMS formation, modeling and detecting experiments of the sensor. The micro-fabrication of the cantilever sensor is processed at a single side (front side) of the silicon wafer, combined with functionalization of a self-assembled monolayer (SAM) on the sensing cantilever for specific molecular capturing. The model of the piezoresistive SiO<sub>2</sub> cantilever sensor is given by using both analysis and simulation, resulting in good agreement with the measuremental data. With the cantilever modified by the specific SAM, the detecting performance of the sensor is experimentally obtained. Attributed to the high sensitivity and the low electric noise of the piezoresistive SiO<sub>2</sub> cantilever, ammonia gas of 0.1 ppm level concentration and dimethyl methylphosphonate vapor of 10 ppb concentration have been well detected. The integrated cantilevers are promising for inexpensive, highly resoluble and portable chemical/biological detection.

## 1. Introduction

Recently, development of miniaturized, inexpensive, ultra-sensitive sensors that are capable of rapidly detecting chemical or biological analyte has been attractive. Among the varieties of developed sensors, micromachined cantilever has been recently researched intensively due to its high sensitivity, portability and low-cost microfabrication [1–5]. This type of bio/chemical micro-sensor can be classified (by operation method) into two kinds, dynamic cantilever and static one. The dynamic cantilever detects resonant frequency shift in terms of specific mass adsorption [3, 5]. For static detection, one side of

the cantilever is coated with a sensing layer that has affinity to the targeted analyte, while the other side is relatively passive. When specific reaction or combination occurs between the analyte and the sensing layer, surface stress will generate on the sensing surface of the cantilever, which gives rise to a bending of the cantilever [1, 2, 4, 5]. The present research is focused on the static bending cantilever sensors for detection of trace chemical vapors.

The specific molecular reaction (or binding) induced cantilever bending can be detected optically or electronically. For on-the-spot portable detection, microcantilevers integrated with on-chip readout are highly in demand. From this point of view, piezoresistive readout is a suitable approach that can

<sup>3</sup> Author to whom any correspondence should be addressed.

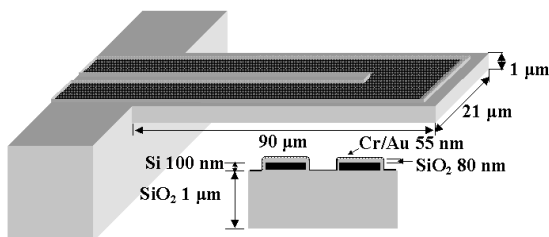


**Figure 1.** Schematic of the piezoresistive  $\text{SiO}_2$  microcantilever, with the dimensions denoted.

measure the bending stress of the cantilever [5–8]. Previously reported piezoresistive microcantilevers for chemical vapor detection comprised either a polysilicon piezoresistor encased in a silicon-nitride cantilever or a doped single-crystalline silicon piezoresistor in a silicon cantilever [9–11]. For the former, the polysilicon piezoresistor is generally with a much lower sensitivity compared to its single-crystalline counterpart [12]. For the latter, p–n junction electric isolation is generally used for the single-crystalline piezoresistors. The electronic noise relative to the p–n junction current leakage is inevitable that more or less lowers the detecting resolution. Moreover, when the silicon cantilevers are constructed very thin to improve the mechanical sensitivity of the cantilever [12], fabrication of ultra-thin piezoresistor is somewhat difficult, as the impurity-doped piezoresistive layer has to be thinner than one half of the cantilever thickness [13].

In the present research we develop a  $\text{SiO}_2$  microcantilever sensor with on-chip built-in piezoresistive readout for highly resolvable detection. The  $\text{SiO}_2$  microcantilever can provide a much higher mechanical sensitivity compared to its silicon or silicon-nitride counterparts, as thermally grown  $\text{SiO}_2$  film features a much lower Young's modulus than single-crystalline silicon or silicon nitride [12, 14]. It can be clearly seen that [15] lists Young's modulus values of thermal  $\text{SiO}_2$ , single-crystalline Si and LPCVD (low pressure chemical vapor deposition)  $\text{Si}_3\text{N}_4$  as 57–79 GPa, 170 GPa and 290–380 GPa, respectively. The high mechanical sensitivity leads to a large surface-stress-induced bending of the cantilever. On the other hand, a very thin single-crystalline silicon layer is employed for piezoresistive detection, which is embedded in the  $\text{SiO}_2$  cantilever. With the piezoresistor fully encapsulated in  $\text{SiO}_2$ , dielectric-film electric isolation instead of negative-biased p–n junction isolation is used in the present research to effectively eliminate current-leakage relative electronic noise. Compared to conventional silicon piezoresistive cantilevers with the p–n junction isolation scheme, the piezoresistive  $\text{SiO}_2$  microcantilever is expected to feature lower electronic noise and, thus, higher signal-to-noise ratio. The piezoresistive  $\text{SiO}_2$  microcantilever is schematically shown in figure 1, with its dimensions denoted. For a transparent view of the cantilever, the specifically self-assembled sensing layer is not shown at the cantilever upper surface.

$\text{SiO}_2$  cantilever-tip probes have been fabricated for AFM (atomic force microscope) applications [14, 16]. Recently a metal-coated  $\text{SiO}_2$  cantilever has been formed for resonant mass-adsorption sensing by using a hard-contact current detection method [17]. These previously reported  $\text{SiO}_2$

cantilevers were constructed with a single layer of a thermally grown silicon-dioxide film. The present research makes an effort to build a  $\text{SiO}_2$  cantilever with a silicon thin layer embedded for piezoresistive self-sensing. The novel cantilever makes full use of the advantages of both  $\text{SiO}_2$  material for high bending sensitivity and the  $\text{SiO}_2$ -encapsulated piezoresistor for low-noise on-chip signal readout.

From the aspect of microfabrication, conventional microcantilevers are normally formed by using a backside release process. Either wet etching or deep reactive ion etching can be used for the backside release. However, the former process generally makes difficulties in protecting the front-side metal interconnection lines from the etching. If the deep dry etching process is used, the expensive process normally leads to a high fabrication cost. In the present work, we develop a single-sided process for fabricating the piezoresistive  $\text{SiO}_2$  microcantilever sensors. All the process steps are implemented from the front side of the SOI (silicon-on-insulator) wafers. The cantilevers can be front-sided released by using gaseous  $\text{XeF}_2$  isotropic etching, thanks to the good etching selectivity between silicon and silicon dioxide. The processes have been found with a high yield and, therefore, a low cost. The etching depth for releasing the cantilevers is almost the same as the cantilever length, i.e. much shallower than the 4 inch wafer thickness.

The model of the piezoresistive  $\text{SiO}_2$  cantilever sensor should be established. The surface stress-induced piezoresistive sensitivity should be calculated for this composite-layer cantilever. In other words, the previously established model for single-layer cantilevers should be modified and adapted to this composite-layer cantilever. Besides, electric-thermal issues should be well treated, due to the different thermal transfer character of the  $\text{SiO}_2$  cantilever from silicon cantilevers. Bimetallic effect of the multi-layer structure should also be considered. The microfabrication, modeling and the detecting experiments will be described in the following sections.

## 2. Fabrication

It is worth pointing out that the geometric design regulation should be obeyed for high-yield fabrication of the  $\text{SiO}_2$  microcantilevers. Reference [16] revealed that the  $\text{SiO}_2$  cantilever fabrication yield can approach 100% as long as the cantilever dimensions are not too large. The paper suggested 25  $\mu\text{m}$  as the upper limit for the cantilever width. In [14], a bending experiment was conducted. Their  $\text{SiO}_2$  cantilever of length 200  $\mu\text{m}$  can deflect up to 100  $\mu\text{m}$ , i.e. shows a satisfactory mechanical flexibility. Our fabrication experiments have shown that the cantilevers not larger than 140  $\mu\text{m}$  in length and 25  $\mu\text{m}$  in width can be high-yield fabricated by using micromachining technologies. The fabricated cantilevers can also be safely operated in both ambient air (for gas detection) and solutions (for specific molecule self-assembly and surface cleaning). In fact, the cantilevers used for the static chemical sensing are unnecessary to be too long. The static bending chemical-sensing cantilevers are not like the cantilevers used for acceleration detection or mass-adsorption resonant sensing. The former can adjust the inertial sensitivity by scaling the cantilever dimensions [18].

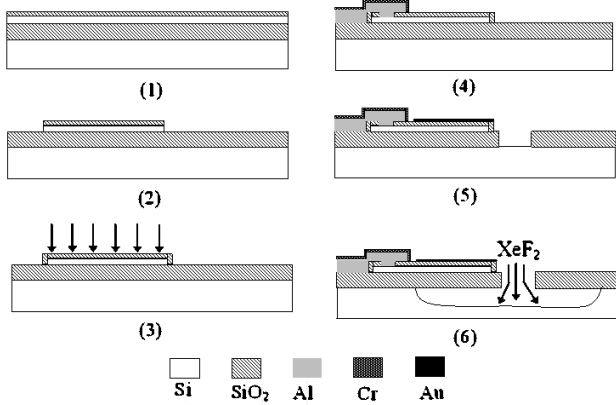


**Figure 2.** Microfabrication steps for the single-side-processed piezoresistive SiO<sub>2</sub> cantilevers.

The latter should locate the mass adsorption site near the cantilever free-end for improving sensitivity [19]. For the bending cantilever sensor, the sensing layer can be coated at the whole upper surface of the sensing cantilever for surface-stress generation while the piezoresistor can also be laid along the whole cantilever for signal readout. Based on the surface-stress sensing mechanism [4], the curvature radius can remain almost unchanged along the whole bending cantilever. Therefore, we finalize the sensing-cantilever dimensions as 90  $\mu\text{m}$  in length and 21  $\mu\text{m}$  in width. The fabricated cantilever sensors are with a high yield, and can well survive environmental vibration and operation in liquid environment.

The single-sided fabrication processes for the cantilevers start from single-sided polished BE-SOI (bonding and etching back silicon-on-insulator) wafers, with a 200 nm thick p-type (100) top layer and a 1  $\mu\text{m}$  thick buried oxide (BOX) layer beneath. The SOI wafer is purchased from Shanghai SIMGUI Technology Co. Ltd. The top layer is first thinned to 135 nm by dry oxidization. With 100 nm thick silicon for the piezoresistor, about 35 nm thick silicon will be further oxidized into SiO<sub>2</sub> to cover the piezoresistor. After the oxide layer removed by BOE (buffered oxide etchant), the following process steps are sketched in figure 2 and described as follows.

- (1) The SOI wafer is dry oxidized to form 50 nm thick SiO<sub>2</sub>. Then the remaining silicon layer is about 113 nm in thickness.
- (2) With photolithography, the etching windows are patterned for the oxide layer and opened by BOE etching, while the photoresist layer serves as the etching mask. Then the U-shaped silicon piezoresistors are formed by aqueous KOH anisotropic etching. The cantilever as well as the piezoresistor is oriented along the  $\langle 110 \rangle$  direction.
- (3) On the top of the existing 50 nm thick SiO<sub>2</sub>, a 30 nm thick SiO<sub>2</sub> layer is grown again by using dry oxidization. The process step consumes about 13 nm thick silicon. After the oxidation, the silicon piezoresistors are fully encapsulated by the SiO<sub>2</sub> layer (including the vertical sides of the silicon resistor). Now the piezoresistor layer is thinned to about 100 nm. To form the piezoresistors, boron ion implantation is processed with the dose of  $3 \times 10^{14} \text{ cm}^{-2}$  and the energy of 35 keV. After ion activation

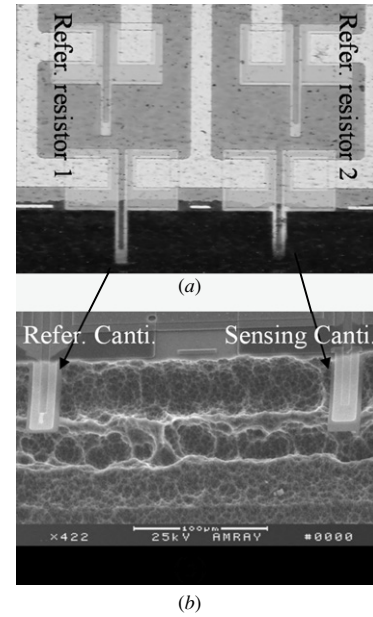


**Figure 3.** (a) Top-view micrograph of the sensor consisting of an on-chip Wheatstone bridge; (b) close-up SEM image showing both the sensing and the referential cantilevers.

at 950 °C for 30 min, the target sheet resistivity is about 200  $\Omega/\square$ .

- (4) The contact holes are opened and, then, interconnection is formed by aluminum sputtering and patterning. After the wafer is annealed in 450 °C nitrogen environment for 30 min, ohmic contact is formed. For protecting the aluminum from damage in the following H<sub>2</sub>SO<sub>4</sub>+H<sub>2</sub>O<sub>2</sub> surface cleaning procedure (see section 4), an extra chromium layer is sputtered and patterned to cover the aluminum lines.
- (5) On the top of a patterned photoresist layer, Cr/Au layers of thickness 5 nm/50 nm are sequentially coated by electron-beam evaporation. Then the Cr/Au pattern on the surface of the sensing cantilever is formed by the lift-off process. From the front side, the SiO<sub>2</sub> cantilevers are shaped by BOE etching with a patterned photoresist as the etching mask. The etching removes the SiO<sub>2</sub> at the surroundings of the cantilever until the silicon substrate beneath the SOI wafer is exposed at the front side.
- (6) To release the SiO<sub>2</sub> cantilevers to free standing, XeF<sub>2</sub> gas-phase etching is processed from the front side of the wafer [20], with a patterned photoresist layer as the etching mask. Since the XeF<sub>2</sub> etching is an isotropic process, the vertical etching depth will be the same as the laterally under-etched distance. As the opening for release is near the end of the cantilever, the lateral under-etch distance almost equals the length of the cantilevers that can be time-controlled with the aid of microscopic inspection.

The top-view micrograph of the fabricated sensor is shown in figure 3(a). For depressing the environmental noise, a Wheatstone bridge is constructed with two piezoresistive cantilevers and two referential resistors located at the supporting frame [7]. One piezoresistive cantilever is a referential cantilever that is configured in the same way as

the sensing cantilever, except that it is 10  $\mu\text{m}$  longer than the sensing cantilever to avoid tuning-fork-like resonance between the two cantilevers. Besides, there is no Cr/Au layer at the referential cantilever surface, which is used on the sensing cantilever for surface modification of the self-assembled monolayer (SAM). Figure 3(b) shows the magnified SEM images of the two cantilevers. By using the concise silicon micromachining fabrication techniques, the cantilever sensors have been measured with a high fabrication yield of about 80%. The highly reproducible cantilevers are also measured with a cantilever-dimensional non-uniformity of smaller than  $\pm 1.5 \mu\text{m}$ .

### 3. Modeling

For calculating the sensitivity of a cantilever composed of a single material, Stoney's equation  $\Delta z = \frac{3L^2(1-\nu)}{Et^2} \Delta\sigma$  has been widely used [4], where  $\Delta z$  represents the free-end displacement of the cantilever. In the expression the cantilever thickness is  $t$ , length is  $L$ , Poisson ratio is  $\nu$ , Young's modulus is  $E$  and  $\Delta\sigma$  is the surface stress at the interfacial surface of the cantilever. However, our piezoresistive silicon-dioxide cantilevers comprise multi-layer materials, with the composite-layer construction schematically drawn in figure 1. Viewed from the profile, the cantilever thickness consists of the Cr/Au layer (5 nm/50 nm), 80 nm thick  $\text{SiO}_2$  layer, 100 nm thick single-crystalline silicon piezoresistive layer and 1  $\mu\text{m}$  thick BOX layer. Stoney's equation should be modified to adapt to the multi-layer cantilever. Sader [21] reported that the application of a differential surface stress to a rectangular plate is equivalent to the free-edge concentrated loading moment of  $\Delta\sigma_s t/2$ . When the cantilever is bent by a uniformly distributed loading surface stress,  $\sigma_s$ , the free-end bending moment is  $M = \Delta\sigma_s t/2$  [21], where  $w$  is the cantilever width. By a linear analysis of small deflection, the radius of the deflective cantilever,  $R$ , can be expressed as

$$\frac{1}{R} = \frac{M}{EI_{\text{eff}}} = \frac{\sigma_s w h_n}{(EI)_{\text{eff}}} \quad (1)$$

where  $(EI)_{\text{eff}} = w \sum_i \left( \frac{E_i}{1-\nu_i} (t_i^3/12 + t_i(h_i - h_n)^2) \right)$  and  $h_n = \left( \sum_i E_i h_i t_i \right) / \left( \sum_i E_i t_i \right)$ . In equation (1),  $E_i$ ,  $\nu_i$ ,  $t_i$  are Young's modulus, Poisson ratio and the thickness of the  $i$ th layer of the cantilever respectively;  $h_i$  is the distance from the top of the cantilever to the middle plane of the  $i$ th layer. The bending stress at the piezoresistive layer can be expressed as

$$\sigma = E_{\text{si}}(h_n - h_t) \frac{1}{R} \quad (2)$$

where  $E_{\text{si}}$  is Young's module of silicon and  $h_t$  is the distance between the upper surface of the cantilever and the middle plane of the thin piezoresistor layer. The relationship between the surface stress and the bending stress can be expressed as

$$\frac{\sigma}{\sigma_s} = \frac{E_{\text{si}} h_n (h_n - h_t)}{(EI)_{\text{eff}}} \quad (3)$$

The defined ratio of  $\sigma/\sigma_s$  represents the mechanical sensitivity of the piezoresistive cantilever in terms of the specific-reaction-induced surface stress. Accordingly, the free-end displacement of the cantilever is

$$\Delta z = \frac{L^2}{2R} = \frac{L^2 w h_n}{(EI)_{\text{eff}}} \quad (4)$$

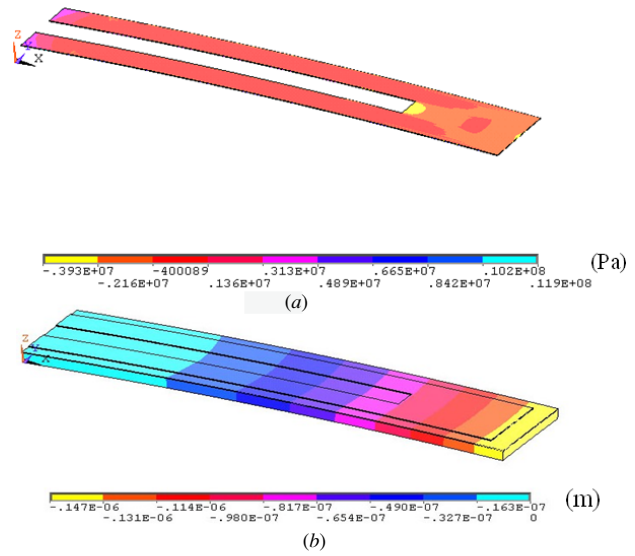


**Figure 4.** FEM simulation results by using ANSYS software. (a) Bending stress distribution in the piezoresistor that is induced by a surface stress of  $1 \text{ N m}^{-1}$ ; (b) bending displacement distribution of the sensing cantilever under the same value of surface stress. (This figure is in colour only in the electronic version)

When the bending stress induced relative resistance changes of the piezoresistor are readout by the Wheatstone bridge, the output voltage can be calculated using

$$V_0 = \frac{V_{\text{in}}(\pi_L - \nu\pi_T)\sigma}{4} = \frac{V_{\text{in}}\sigma_s E_{\text{si}} h_n (h_n - h_t)}{4(EI)_{\text{eff}}} \quad (5)$$

where  $V_{\text{in}}$  is the supply voltage of the bridge, and  $\pi_L$  and  $\pi_T$  are the longitudinal and transversal piezoresistive coefficients respectively. Using this model, the sensitivity of the designed cantilever can be calculated as  $\sigma_s^{-1}\sigma = 2.72 \times 10^6 \text{ (m}^{-1}\text{)}$ ,  $\sigma_s^{-1}\Delta R/R = 8.37 \times 10^{-4} \text{ (m N}^{-1}\text{)}$  or  $\Delta z = 1.47 \times 10^{-7} \sigma_s \text{ (m)}$ , respectively. Here the piezoresistive coefficient of  $\pi_{44} \approx 100 \times 10^{-11} \text{ Pa}^{-1}$  is used for calculation.

FEM (finite elements method) simulation is also implemented by using ANSYS-7.0 software, with the results shown in figure 4. The results are obtained by applying the  $1 \text{ N m}^{-1}$  surface stress on the surface of the sensing cantilever. A pre-stressed ultra-thin layer of thickness 2 nm (with a similar effective thickness to the stressed SAM-target interface layer) is built on the top surface of the cantilever to generate the desired surface stress in both the longitudinal and the transverse directions of the cantilever. Young's modulus of 73 GPa is used for the thin layer, which is simply assumed to be identical to that of the beneath Au layer. Unlike the theoretical analysis shown above, where one-dimensional approximation is done for the cantilever, the surface stress applied for the FEM simulation is along both the length and the width directions of the cantilever. As shown in figure 4(a), the surface-stress-induced bending stress at the piezoresistive layer is uniformly distributed. The mechanical sensitivity of the sensing cantilever is simulated as  $\sigma_s^{-1}\sigma \approx 2.2 \times 10^6 \text{ (m}^{-1}\text{)}$  and  $\Delta z \approx 1.5 \times 10^{-7} \sigma_s \text{ (m)}$ , respectively. The simulation results agree well with the theoretical analysis that is based on the multi-layer cantilever model. In contrast, if the single-layer model analysis is used, i.e. only a silicon-dioxide layer is taken into consideration, Stoney's equation will give the

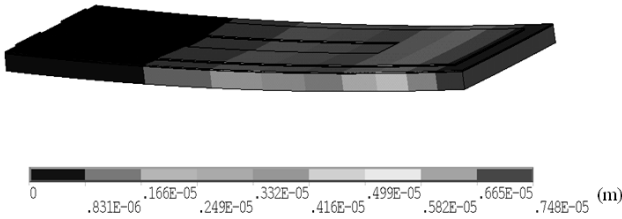


**Figure 5.** Simulated initial bending of the multi-layer cantilever caused by thermal mismatch stress in the BOX layer.

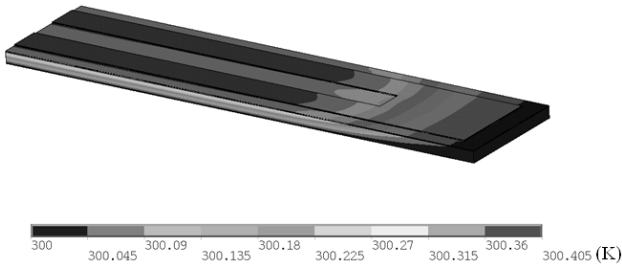


**Figure 6.** Simulated temperature distribution along the sensing cantilever, when it is heated by 100 mV power supply.

sensitivity as  $\Delta z = 2.7 \times 10^{-7} \sigma_s$ , which is far different from the simulation result. Therefore, it can be seen that the multi-layer cantilever model is suitable for designing the piezoresistive SiO<sub>2</sub> cantilever sensors.

Comprising the main part of the cantilever thickness, the BOX layer was grown by wet oxidation at 1100 °C, prior to the wafer bonding process to form the SOI wafers. Since the oxide layers on the top of the silicon piezoresistive layer is much thinner than this BOX layer, the initial bending status of the cantilever will be mainly determined by the stress built in the BOX layer (the single-crystalline piezoresistive silicon layer is free of stress). The BOX layer suffers compressive stress that comes out of the thermal mismatch between silicon and silicon dioxide. Therefore the released cantilever has to bend up, as shown in the SEM image of figure 3(b). Based on bimetallic effect theory [22], the free-end bending deflection of the referential cantilever is calculated as about 5.7 μm. As shown in figure 5, FEM simulation is also implemented, resulting in a displacement of 6–7 μm at the cantilever free end, where the BOX-layer thermal mismatch stress is introduced in all directions.

As encapsulated in the insulating SiO<sub>2</sub> cantilever, the silicon piezoresistor is easy to be heated up when electric current flows through the resistor. Upon the cantilever being heated by the supplied voltage, the temperature distribution along the cantilever is obtained by FEM simulation, with the results illustrated in figure 6. When the piezoresistor of the sensing cantilever is heated by 100 mV applied voltage (corresponding to 200 mV power supply to the whole Wheatstone bridge), the simulated temperature distribution along the cantilever length is quite uniform, with the temperature non-uniformity not larger than 0.41 °C. Therefore, it is reasonable to use an average temperature to represent the whole cantilever. The relationship between the voltage supply to the sensing cantilever (including the Cr/Au surface coating layer) and the average cantilever temperature is obtained by

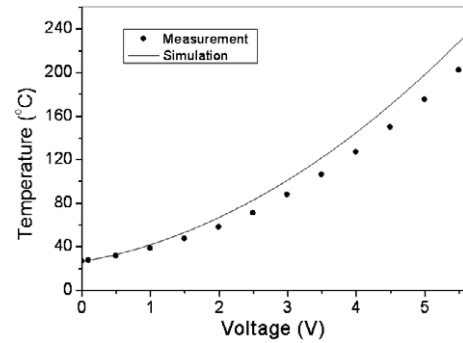


**Figure 7.** The relationship between the supplied voltage to the Wheatstone bridge and the average temperature of the piezoresistor in the sensing cantilever is obtained by both measurement and simulation.

both measurement and simulation. As shown in figure 7, the cantilever temperature will significantly increase with increasing voltage. The two results have a slight mutual deviation since only thermal transfer from the cantilever to the frame is considered in the simulation. Based on the results, the power supply to the cantilever sensor is finalized as 200 mV, i.e. one piezoresistor is supplied with 100 mV. Under the supply voltage, the electric-heating-induced temperature increase of the cantilever can be slightly smaller than 0.5 °C.

It is worth pointing out that, using a temperature adjustable oven, the resistance versus temperature was previously measured and calibrated for both the two piezoresistors in the cantilevers and the two referential resistors at the substrate frame. For the referential resistors located at the supporting frame, the resistance change only comes out of the temperature change. On the other hand, the resistance change in the piezoresistors is induced by both the temperature change and the temperature-change-induced bimetallic effect. The heating-induced bimetallic bending of the cantilever in turn causes a piezoresistive output. Figure 8 shows the measured resistance change in terms of temperature for both the piezoresistor in the sensing cantilever and the referential resistor at the frame substrate. By subtracting the normalized resistance of the referential resistor from that of the piezoresistor, the obtained difference in resistance should come from the bimetallic effect as well as the temperature difference between the cantilever and the supporting substrate. Under the Wheatstone-bridge power supply of 200 mV, the temperature difference is about 0.5 °C due to the above-mentioned electric-heating effect on the piezoresistive cantilever. For eliminating the influence from the 0.5 °C temperature difference, the calibrated resistance value of the referential resistor used for the calculation is always 0.5 °C lower than the temperature of the cantilever resistor. In this way, the bimetallic bending-induced piezoresistive change is finally obtained as  $(\Delta R_{\text{Bimetallic}}/R_0)/\Delta T \approx -0.032\% \text{ } ^\circ\text{C}^{-1}$  (shown in figure 8). FEM simulation is also conducted to evaluate the bimetallic bending versus temperature. A slightly larger result of  $(\Delta R_{\text{Bimetallic}}/R_0)/\Delta T = -0.049\% \text{ } ^\circ\text{C}^{-1}$  is simulated and also illustrated in figure 8. As the electric-heating-induced cantilever temperature increase is only about 0.5 °C, the bimetallic effect induced surface stress can be

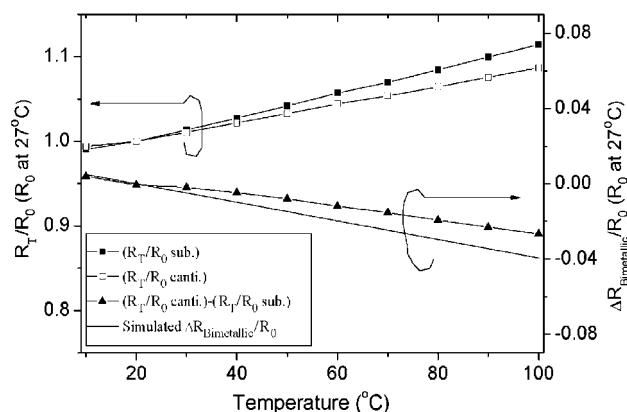


**Figure 8.** Normalized resistance change in terms of temperature is measured for both the piezoresistor in the sensing cantilever and the referential resistor at the frame substrate. By subtracting the resistance of the referential resistor from that of the piezoresistor, the obtained resistive difference represents the resistance variation induced by bimetallic effect of the multi-layer cantilever. The bimetallic bending induced piezoresistive change is obtained as about  $-0.032\% \text{ } ^\circ\text{C}^{-1}$  that is comparable to the simulated result of about  $-0.049\% \text{ } ^\circ\text{C}^{-1}$ .

calculated as only about  $0.20 \text{ N m}^{-1}$ . With the Wheatstone bridge scheme, this zero-point offset can be further cancelled off by the referential piezoresistive cantilever.

#### 4. Experiments

The fabricated sensor chip is packaged together with a linear amplifier for signal conditioning. As analyzed in the last section, the supply voltage to the Wheatstone is chosen as 200 mV. During the measurement, the sensor output voltage is fed into a data acquisition instrument (Cbook/2001) and recorded by a personal computer. The data acquisition frequency is set as 10 Hz.

The sensing experiment is performed on a MF-4 dynamics gas-mixing apparatus that is made by Chinese National Research Center for Certified Reference Materials. In the vapor detecting experiment, two kinds of reference gases (ammonia gas and DMMP standard gases) are purchased from the Nanjing Mucop Nanfen Special Gas Co. The purchased gas is with an initial concentration in nitrogen. A further diluted gas flow can be obtained by proportionally mixing the reference gas flow with a purified  $\text{N}_2$  flow. During the experiment, the cantilever sensor is placed into a testing cell (with 200 mL volume). A four-way valve is used to switch between the target gas and another purified nitrogen gas for cleaning. The gas flow through the testing cell is with a fixed rate of  $2.0 \text{ L min}^{-1}$ .

The gas supplier executes a very strict quality control procedure on the gas purification. According to the specification sheets provided by the manufacturer, the purity of both the ammonia gas and the DMMP standard gas has been examined to be higher than 99%. Unlike the purchased ammonia gas that has been used by us and many other users for a long period of time, the DMMP gas has been purchased by us for the first time. Therefore, we perform a GC/MSD analysis on the provided DMMP gas. In the obtained total ion

chromatography and corresponding mass spectroscopy, only one peak of DMMP is observed that evidences that the purity of the DMMP standard gas is high enough. Both the purified gas and the testing setup described above can effectively avoid any non-specific binding of trace gases involuntarily introduced into the system.

For chemical sensing, a sensitive coating should be located at the top side of the sensing cantilever. Modification of the sensing cantilever with a functionalized coating is quite essential for the cantilever-based sensors. Basically, thioliates with a functionalized tail group can be self-assembled on the Au-coated surface of the cantilever, which acts as a sensitive coating or the first layer to immobilize another layer of molecular specific substance. A SAM of 11-mercaptoundecanoic acid (11-MUA) is used in the present research. Before the SAM functionalization, the Au film on the sensing cantilever is sequentially cleaned in acetone, absolute ethanol, deionized water and piranha solution (7:3  $\text{H}_2\text{SO}_4$  98%/  $\text{H}_2\text{O}_2$  31%). The sensor chip is then immersed into a 1 mM solution of 11-MUA in ethanol for 16 h to form the 11-MUA modified cantilever. Then the cantilever is rinsed twice with ethanol to remove non-specific adsorption. After dried at ambient air for hours, the cantilever sensor is ready for ammonia gas detection.

In our experiments, the self-assembling process of the 11-MUA on the cantilever is monitored online and recorded with the piezoresistive sensor. During the self-assembling process, the response voltage continues with a negative value. After the voltage is saturated, we consider that the SAM growing is completed. The growth of the thioliates on the Au surface results in a tensile surface stress (denoted by the negative offset output of the sensor) and, thus, leads to a downward bending of the cantilever. From the output voltage, we find that the SAM growing causes a surface stress of about  $0.4 \text{ N m}^{-1}$ . For this reason, the SAM growing process can somewhat compensate for the initial up-bending of the cantilever by the fore-mentioned bimetallic effect. Attributed to the silicon piezoresistors encapsulated and insulated by  $\text{SiO}_2$ , no obvious current leakage can be detected between two adjacent Wheatstone bridges when they are packaged together and put in ambient air. Moreover, the electric signal noise as low as  $0.3 \mu\text{V}$  is measured during the online monitored SAM growing that is processed in the 11-MUA ethanol solution.

We expect that the 11-MUA can be used as a sensitive coating to capture the ammonia gas via hydrogen bonding. The response of the SAM-modified sensor to various concentrations of ammonia gases is measured and shown in figure 9. At each concentration of either 1 ppm or 25 ppm, the sensor is continuously tested for three times within 20 min. The sensor shows satisfactory rapidity, repeatability and reversibility. The satisfactory dynamic equilibrium between specific adsorption and desorption should be attributed to the SAM of 11-MUA. Besides, the signal noise level of the sensor in the experiments is found to be about  $0.3 \mu\text{V}$ , while the response output to 1 ppm ammonia gas is about  $7 \mu\text{V}$ . Therefore, the noise-limited resolution of ammonia gas detection can be reasonably estimated at a level of 0.1 ppm.

The developed cantilever sensors are then used for detection of trace sarin vapor. The use of chemical warfare agents as the measure of terrorism has become a real existing

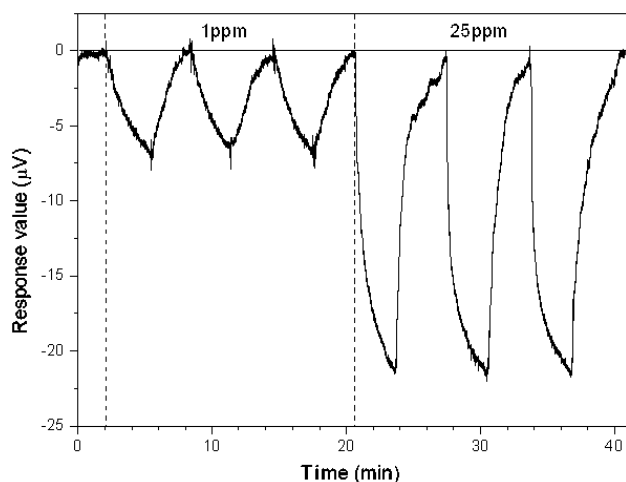


**Figure 9.** Repeatable response of the 11-MUA functionalized cantilever sensor to ammonia gas of ultra-low concentrations of 1 ppm and 25 ppm is sequentially obtained experimentally. The noise-limited resolution is estimated at about 0.1 ppm level.

threat. The Tokyo Subway sarin attack in 1995 has heightened the awareness of the public. Since the chemical warfare agents, especially the nerve agents, are highly toxic, early alarm and sensitive detection of these agents are of great importance. For assessment of sarin sensors in ordinary labs, the studies on detecting the nerve agent of sarin frequently use nontoxic DMMP (dimethyl methylphosphonate) as the stimulant gas due to its similar molecular characters to sarin.

For specific adsorption of DMMP, we further modify the SAM of 11-MUA with Cu<sup>2+</sup>. The 11-MUA/Cu<sup>2+</sup> composite layer is used as the sensitive coating to capture organophosphorus molecules. This composite layer can specifically recognize P=O containing compounds, owing to the formation of the P=O–Cu<sup>2+</sup> coordination structure on the surface [23]. After the 11-MUA modification process described above, the cantilever is immersed in a 2 mM CuSO<sub>4</sub>·5H<sub>2</sub>O aqueous solution for 1 h to yield the composite layer of 11-MUA/Cu<sup>2+</sup>. The sensing experiment has approved that the adsorption of organophosphorus DMMP compound on the 11-MUA/Cu<sup>2+</sup> self-assembled bi-layer can produce the surface stress at the surface of the cantilever for recognizing the DMMP in the trace level. As shown in figure 10, the cantilever sensor shows rapid detecting capability to various DMMP concentrations. For the 200 ppb concentration (equivalent to about  $1 \times 10^{-3}$  mg L<sup>-1</sup>), the sensor response signal gets its saturation within 5 min. After the testing period of 6 min, pure nitrogen gas is switched for cleaning the testing cell. About 8 min is needed for the signal recovery. For the ultra-low concentration of 20 ppb (equivalent to about  $1 \times 10^{-4}$  mg L<sup>-1</sup>), the sensing signal can be saturated within 4 min and recovered within 6 min. Using the present gas generating apparatus, we cannot get a lower concentration with a satisfactory mixing accuracy. From the signal noise floor, better than 10 ppb (equivalent to about  $5 \times 10^{-5}$  mg L<sup>-1</sup>) sensing resolution to DMMP can be estimated. This rapidly reversible response of the sensor to DMMP can be attributed to the moderate covalent-specific bonding mechanism. Unlike the very strong biological-specific binding, where the highly specific bio-molecular binding is formed at multiple points,

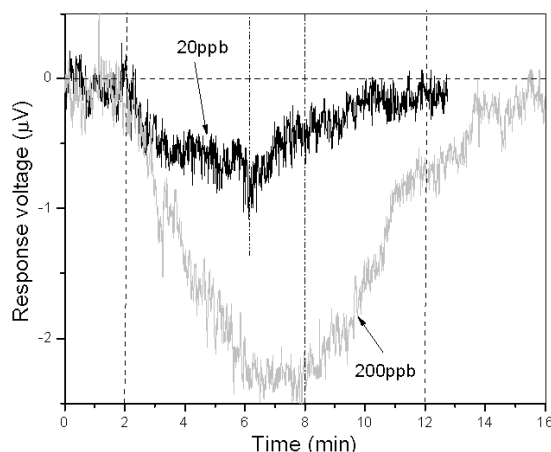


**Figure 10.** The sensor response to trace DMMP vapor is measured for concentrations of 200 ppb and 20 ppb, respectively. The noise-limited detecting resolution is better than 10 ppb (equivalent to about  $5 \times 10^{-5}$  mg L<sup>-1</sup>).

the chemical vapor sensing is based on a single-point bond-coordination mechanism. The single-point bond coordination has a moderate strength that leads to the reversible response of this type of chemical gas sensors [24, 25].

## 5. Conclusions

This paper focuses on the construction, micro-fabrication, modeling analysis and sensing experiment of a novel piezoresistive SiO<sub>2</sub> microcantilever sensor for high-resoluble chemical gas detection. The proposed cantilever sensor features high sensitivity due to the low Young's modulus of silicon dioxide and low electric noise because of the piezoresistor being fully encapsulated in the insulating SiO<sub>2</sub>. The sensor is high-yield fabricated by using a single-side-processed micromachining technique. With the functionalization of the specific self-assembled monolayer (or bi-layer) on the surface of the sensing cantilever, the sensors have been experimentally approved being able to detect ammonia gas and DMMP vapor at ultra-low concentration levels of 0.1 ppm and 10 ppb, respectively. Featuring high resolution and rapid response, the piezoresistive SiO<sub>2</sub> cantilever sensor is promising to become a micromachined platform for on-the-spot trace gaseous detection.

## Acknowledgments

This research is supported by projects of the National Basic Research Program of China (2006CB300405) and the National Scientific Foundation of China (60376038).

## References

- [1] Berger R, Delamarche E, Lang H P, Gerber C, Gimzewski J K, Meyer E and Guntherodt H J 1997 Surface stress in the self-assembly of Alkanethiols on gold *Science* **276** 2021–4
- [2] Fritz J, Baller M K, Lang H P, Rothuizen H, Vettiger P, Meyer E, Guntherodt H J, Gerber C and Gimzewski J K 2000 Translating biomolecular recognition into nanomechanics *Science* **288** 316–8

- [3] Hagleitner C, Hierlemann A, Lange D, Kummer A, Kerness N, Brand O and Baltes H 2001 Smart single-chip gas sensor microsystem *Nature* **414** 293–6
- [4] Thundat T, Warmack R J, Chen G Y and Allison D P 1994 Thermal and ambient-induced deflections of scanning force microscope cantilevers *Appl. Phys. Lett.* **64** 2894–6
- [5] Lavrik N V, Sepaniak M J and Datskosa P G 2004 Cantilever transducers as a platform for chemical and biological sensors *Rev. Sci. Instrum.* **75** 2229–53
- [6] Tortonese M, Barrett R C and Quate C F 1993 Atomic resolution with an atomic force microscope using piezoresistive detection *Appl. Phys. Lett.* **62** 834–6
- [7] Thaysen J, Boisen A, Hansen O and Bouwstra S 2000 Atomic force microscopy probe with piezoresistive read-out and a highly symmetrical Wheatstone bridge arrangement *Sensors Actuators A* **83** 47–53
- [8] Rasmussen P A, Thaysen J, Bouwstra S and Boisen A 2001 Modular design of AFM probe with sputtered silicon tip *Sensors Actuators A* **92** 96–101
- [9] Kooser A, Gunter R L, Delinger W D, Porter T L and Eastman M P 2004 Gas sensing using embedded piezoresistive microcantilever sensors *Sensors Actuators B* **99** 474–9
- [10] Jensenius H, Thaysen J, Rasmussen A A, Veje L H, Hansen O and Boisen A 2000 A microcantilever-based alcohol vapor sensor-application and response model *Appl. Phys. Lett.* **76** 2615–7
- [11] Pinnaduwege L A *et al* 2004 A sensitive, handheld vapor sensor based on microcantilevers *Rev. Sci. Instrum.* **75** 4554–7
- [12] Bao M H 2000 Micro mechanical transducer *Handbook of Sensors and Actuators* ed S Middelhoek (Amsterdam: Elsevier)
- [13] Harley J A and Kenny T W 1999 High-sensitivity piezoresistive cantilevers under 1000 Å thick *Appl. Phys. Lett.* **75** 289–91
- [14] Tang Y, Fang J, Yan X and Ji H 2004 Fabrication and characterization of SiO<sub>2</sub> microcantilever for microsensor application *Sensors Actuators B* **97** 109–13
- [15] MEMS and Nanotechnology Clearinghouse/material database <http://www.memsnet.org/material>
- [16] Albrecht T, Akamine S, Carver T and Quate C 1990 Microfabrication of cantilever styli for the atomic force microscope *J. Vac. Sci. Technol. A* **6** 3366–96
- [17] Dohn S, Hansen O and Boisen A 2006 Cantilever based mass sensor with hard contact readout *Appl. Phys. Lett.* **88** 264104
- [18] Dong J, Li X, Wang Y, Lu D and Ahat S 2002 Silicon micromachined high shock accelerometers with curved-surface-application structure for over-range stop protection and free-mode-resonance depression *J. Micromech. Microeng.* **12** 742–6
- [19] Jin D, Li X, Liu J, Zuo G, Wang Y, Liu M and Yu H 2006 High-mode resonant piezoresistive cantilever sensors for tens-femtogram resolvable mass sensing in air *J. Micromech. Microeng.* **16** 1017–23
- [20] X Li, Takahito Ono, Y Wang and Masayoshi Esashi 2003 Ultrathin single-crystalline-silicon cantilever resonators: fabrication technology and significant specimen size effect on Young's modulus *Appl. Phys. Lett.* **83** 3081–3
- [21] Sader J E 2001 Surface stress induced deflections of cantilever plates with applications to atomic force microscope: rectangular plates *J. Appl. Phys.* **89** 2911–21
- [22] Barnes J R, Stephenson R J, Woodburn C N, O'Shea S J, Welland M E, Raymand T, Gimzewski J K and Gerber G 1994 A femtojoule calorimeter using micromechanical sensors *Rev. Sci. Instrum.* **65** 3793–8
- [23] Crooks R M, Yang H C, McEllistrem L J, Thomas R C and Ricco A J 1997 Interactions between self-assembled monolayers and an organophosphonate *Faraday Dis.* **107** 285
- [24] Pinnaduwege L, Boiadjev V, Hawk J and Thundat T 2003 Sensitive detection of plastic explosives with self-assembled monolayer-coated microcantilevers *Appl. Phys. Lett.* **83** 1471–3
- [25] Pinnaduwege L, Thundat T, Hawk J, Hedden D, Britt P, Houser E, Stepnowski S, McGill R and Bubb D 2004 Detection of 2,4-Dinitrotoluene Vapor Using Microcantilevers *Sensors Actuators B* **99** 223–9